Molecular dynamics simulation of hydrogen and helium trapping in tungsten

Petr Grigorev[a,b,c,*], Aleksandr Zinovev[a,d,e], Dmitry Terentyev[a], Giovanni Bonny[a], Evgeny E. Zhurkin[c], Guido Van Oost[b], Jean-Marie Noterdaeme[f]

[a] *SCK•CEN, Nuclear Materials Science Institute, Boeretang 200, Mol, 2400 Belgium*
[b] *Ghent University, Applied Physics EA17 FUSION-DC, St.Pietersnieuwstraat 41, Gent, B4 B-9000 Belgium*
[c] *Department of Experimental Nuclear Physics K-89, Institute of Phydics, Nanotechnologies and Telecommunications, Peter the Great St.Petersburg Polytechnic University, St. Petersburg, Russia*
[d] *Université catholique de Louvain, Place de l'Université 1, B-1348 Louvain-la-Neuve, Belgium*
[e] *Institute for Metals Superplasticity Problems, Russian Academy of Sciences, ul. S. Khalturina 39, Ufa, 450001 Russia*
[f] *Max-Planck-Institut für Plasmaphysik, Garching, Germany*

Abstract

Tungsten has been chosen as the divertor armour material in ITER and is the main candidate material for plasma-facing components for future fusion reactors. Interaction of plasma components with the material is unavoidable and will lead to degradation of the performance and the lifetime of the in-vessel components. On top of that special attention is drawn to tritium retention in the reactors vessel from safety point of view, since tritium is a toxic and radioactive material. In order to gain better understanding of the mechanisms driving accumulation of plasma components in the material and subsequent degradation of the material, atomistic simulations are employed. The focus of this work is on so-called self trapping of H and He atoms or, in other words, Frenkel pair formation in bulk tungsten in the presence of H and He atoms. Two versions of a model embedded atom interatomic potential and a bond order potential were tested by comparing it with *ab initio* data regarding the binding properties of pure He and He-H-Vacancy clusters and energetics of Frenkel pair formation. As a result of Molecular Dynamics simulations at finite temperature

*Corresponding author

the values of critical H concentration needed for generating a Frenkel pair in the presence of He clusters were obtained. The results show that the critical H concentration decreases with the size of He cluster present in the simulation cell and thus, Frenkel pair formation by H is facilitated in the presence of He clusters in the material.
Keywords: tungsten, plasma facing material, hydrogen retention, helium, molecular dynamics

1. Introduction

Plasma-facing materials in a fusion device are exposed to extreme conditions in terms of heat and particle loads as well as to high energy neutron irradiation. As a consequence of the fact that plasma-facing materials are in direct contact with plasma, a failure of the material can lead to a catastrophic event for the device. Due to its outstanding thermal properties, tungsten (W) was chosen as the divertor armour material for ITER - the next generation tokamak that is currently under construction, and DEMO - future demonstration nuclear fusion power station [1].

Together with demonstration and testing the technologies for DEMO, one of the main goals of operation of ITER is to demonstrate the control of fusion plasma with negligible consequences for the environment. From this point of view special attention is drawn to tritium (T), which is a toxic and radioactive hydrogen (H) isotope and is a part of the fusion fuel. Consequently, the retention of T in the plasma-facing material is a safety issue, hence a limit of 700 g of T accumulated in the reactor chamber was set for ITER by the safety authorities [2]. Helium (He) is produced in fusion reactions inside the plasma and also in transmutation reactions of W caused by high-energy neutrons being a product of the fusion reaction. Thus, both T and He will be present in the material during the device operation. Therefore it is important to investigate possible synergetic effects between T and He both in terms of T retention and possible detrimental effects on the properties of the plasma facing material.

The effect of H plasma exposure on W has been extensively studied in experiments involving deuterium plasma [3–11]. H concentration can easily exceed the solubility limit in the subsurface area during high flux plasma exposure. This leads to H bubble and void formation occurring at a depth of several μm, which exceeds the implantation depth of a few nm. Experiments involving He implantation demonstrate the presence of He bubbles and 'fuzz' formation at a length scale comparable to the implantation depth [12–14].

However systematic studies are scarce and large scattering of the data is usually attributed to different material preparation procedures, material microstructure and impurity levels in different experiments [8]. Experimental studies involving simultaneous H and He plasma exposure [15, 16] demonstrated suppressed blister formation as compared to pure H plasma exposure. This effect was attributed to a decrease of H permeability through the subsurface region due to He bubble formation. Another remarkable effect was the detection of nanometric He bubbles at a depth significantly larger than the He implantation range [15], not seen in pure He exposures.

H and He behaviour in W has been also investigated by means of atomistic simulations, a thorough review of recent modelling activities can be found in [17]. According to *ab initio* studies both H and He atoms occupy tetrahedral interstitial position in bulk W with a very low migration barrier between the positions [18–21]. At the same time clustering behaviour of H or He atoms in bulk W is essentially different: H atoms show practically zero interaction while He atoms exhibit strong binding leading to so-called self-trapping He bubble formation mechanism [22]. *Ab initio* studies [22–24] showed that there is an attractive interaction between He clusters and H atoms in bulk W. However, comprehensive physical mechanisms leading to synergetic effects during simultaneous H and He plasma exposure are not clear so far.

In the present work, the H bubble nucleation in W in the presence of $\mathrm{He_M}$ (M - number of atoms in the cluster) clusters in the material was assessed by means of Molecular Static (MS) and Molecular Dynamics (MD) simulations. The effects of the H implantation rate and the size of $\mathrm{He_M}$ clusters (M) present in the

system on H bubble nucleation were investigated. The obtained MS results were compared with *ab initio* data in order to validate the choice of the interatomic potential. MD simulations allowed one to detect and investigate the conditions for H bubble nucleation in terms of critical H concentration depending on the content of He in the system. This study gives an insight about mechanisms of H bubble formation during mixed He-H plasma exposure and, together with the data for diffusion and thermal stability of mixed He_M-H_N clusters reporter earlier [25], provides the parameters needed for higher scale models giving the opportunity for full scale plasma exposure simulations.

2. Computational details

The Molecular Static calculations were performed using interatomic potentials for the W-H-He system developed in the frameworks of two different models: Bond Order Potentials (BOP) by Li *et. al.* [26, 27] and Embedded Atom Method (EAM) developed by Bonny *et. al.* [28]. The BOP potential was fitted with special attention on reproducing defect formation energies and interaction of H and He with the defects. Both EAM potentials were created aiming for the investigation of the interaction of H and He with dislocations in tungsten and are based on the interatomic potential for W-W interaction named "EAM2" by Marinica *et. al.* [29].

The base W-W potential was selected after critical review of 19 different EAM potentials with special attention to properties of screw dislocations given in [30]. There are two different versions of the EAM potential, referred to as "EAM1" and "EAM2" in [28].

For the EAM1 potential, emphasis was put on a quantitative reproduction of *ab initio* data for the binding between H-H, He-He and He-H pairs in the bulk tungsten. The off-centre position of a H atom in a vacancy as predicted by Density Functional Theory (DFT) [19] was not considered, and therefore both H and He are described by pair potentials only.

For EAM2 the focus was made on stabilising a H atom in an off-centre

position in the vacancy and therefore an embedding function was added for H. All types of the potentials predict the tetrahedral position for a H atom as the most favourable in bulk W. The main goal of the MS calculations was to compare and validate the interatomic potentials with *ab initio* data available in literature and choose the potential for further Molecular Dynamic simulations at finite temperature.

The size of the crystallite used in the simulations was $10\times10\times10$ a_0^3 (a_0 is the lattice constant predicted by the potential: 3.14 and 3.165 $\mathring{A}$ for EAM and BOP potentials respectively). It contained 2000 atoms before any point defect or cluster was introduced. Periodic boundary conditions were applied in all three directions. The incremental binding energy of H or He atom to $\mathrm{He_M}$ or $\mathrm{He_M}$-H-Vac cluster is defined as an energy difference between the system *1* where a H or He atom (A) is part of the cluster (C) and a system *2* where the gas atom is far away from the cluster and can be written as:

$$E_b(\mathrm{AC}) = E_{tetra}(\mathrm{A}) + E(\mathrm{C}) - E(\mathrm{AC}) - E_{ref} \tag{1}$$

where $E_b(\mathrm{AC})$ is the total energy of the system *1*, $E_{tetra}(\mathrm{A})$ - energy of the system with H or He atoms in tetrahedral interstitial position, $E(\mathrm{C})$ is the energy of the system with a cluster and E_{ref} is added to complete the energy balance. In this notation a positive value indicates attraction and a negative value indicates repulsion.

The so-called process of self-trapping and defect formation during plasma implantation can be seen as a $\mathrm{He_M}$ cluster formation, and a consequent generation of a Frenkel pair (vacancy and self interstitial pair) assisted by the cluster. The Frenkel pair formation energy $E_f(FP)$ was studied by means of Molecular Static calculations and was estimated via calculating the following energy balance:

$$E_f(\mathrm{FP}) = E(\mathrm{He_M\text{-}Vac}) + E(\mathrm{SIA}) - E(\mathrm{He_M}) - E_{ref} \tag{2}$$

where $E(\mathrm{He_M\text{-}Vac})$ is the total energy of the box containing the $\mathrm{He_M}$ cluster

in a vacancy, $E(\mathrm{He_M})$ and $E(\mathrm{SIA})$ is total energy of the system containing a $\mathrm{He_M}$ cluster and a Self Interstitial Atom (SIA) in the form of a $\langle 1\,1\,1 \rangle$ crowdion in bulk tungsten respectively, E_{ref} is the total energy of the box containing no defects (BCC W in our case). In this notation, a positive value of the formation energy corresponds to an endothermic process, i.e. a certain activation energy is necessary to create a Frenkel pair. Negative value of formation energy corresponds to an exothermic process, i.e. energy is released during the reaction. The static relaxation was performed using the conjugate gradient algorithm embedded in LAMMPS simulation package [31] with a stopping criterion on the relative energy change of 10^{-10} between minimisation steps. Prior to the static relaxation of the considered atomic configuration a short MD run at 300 K for 1 ps was performed after which the system was quenched to 0 K. This procedure allows the possibility for the system to evolve out of local minima and arrange itself into the most stable configuration.

The computational cell for MD simulations was a cube $10{\times}10{\times}10\ a_0^3$ in which the crystal's $\langle 1\,0\,0 \rangle$ directions were aligned with the coordinate axes. Periodic boundary conditions were applied in all three directions. The needed number of He atoms (M) were assigned random positions in the crystal from the very beginning, and H atoms were added in the computation cell in random positions with certain periodicity. The temperature was kept constant equal to 800 K in all the simulations. The value of the temperature was chosen to ensure high mobility of the clusters during the simulations and corresponds to surface temperature range at divertor vertical targets during ITER baseline heat load scenario as predicted in [32]. The interatomic potential "EAM2" and NVT ensemble were used.

Two series of simulations were conducted: the first one was directed to study the effect of hydrogen income periodicity (HIP) on the ejection process. In this case no He atoms were present, and the HIP varied from 10 to 90 ps/atom. In order to promote the ejection process, a tungsten atom was removed from the initial configuration, forming a vacancy. In the second series the effect of the initial He atom number on the moment of the first tungsten atom ejection was

investigated in the defect-free lattice. The initial number of He atoms varied from 0 to 6, the HIP was equal to 30, 50 or 90 ps/atom. Given the size of the simulation box the corresponding particle flux is $\approx 10^{29}$ $\frac{1}{m^2 s}$ which is five orders of magnitude higher than the expected flux in ITER and accessible by the experiments. However due to the limitations of MD, lower values of the flux are not feasible.

In order to detect an atom ejection (Frenkel pair formation), the positions of the tungsten atoms in the simulation box were periodically compared with the corresponding ideal lattice during the post-processing stage. A lattice site was considered empty if a sphere of radius equal to 0.2 a_0, encircled around the site, did not contain any tungsten atoms. The sphere radius was chosen to be slightly larger than the typical thermal oscillation amplitude, measured in a separate MD simulation. If the sphere remained empty during 80 % of a 300 ps timespan, the corresponding tungsten atom was assumed to have been ejected and the lattice site was considered as "vacant", to filter out occasional leaps of tungsten atoms from their positions.

The atomic concentration of H in the simulation box in that moment serves as a measure of the ease of atom ejection and is called "critical average hydrogen concentration" in the present text. "Critical local hydrogen concentration" was calculated for several simulations as well, meaning the number of hydrogen atoms within a sphere of radius equal to a_0 encircled around the vacant lattice site at the moment of tungsten atom ejection, divided by the sphere volume.

3. Results and discussion

3.1. Molecular Static results

A number of MS calculations was done in order to test the performance of the interatomic potentials before launching more computationally demanding dynamic simulations. Three main processes that define the trapping during mixed He-H implantation are: stability of He_M clusters, stability of mixed He_M-H_N clusters and Frenkel pair formation in the presence of He_M clusters.

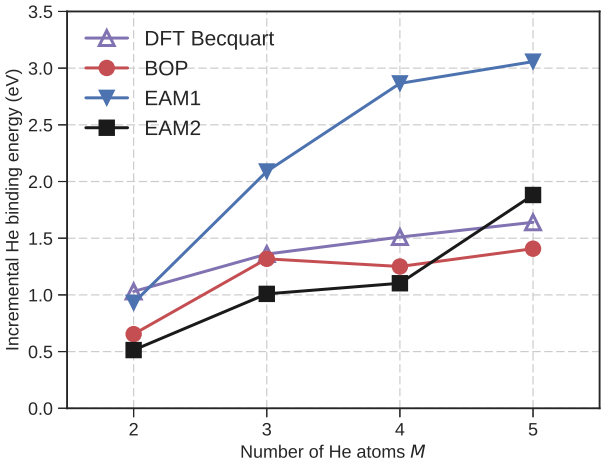

Figure 1: Incremental binding energy of a He atom to a He_M cluster in bulk tungsten

The performance of the potentials regarding these three processes was assessed by calculating the incremental binding energy of a pure He_M cluster, binding energy of a H atom to He_M-H-Vac clusters and Frenkel pair formation energy and comparison of the results with *ab initio* data from the literature.

The results of the potentials for the binding energy of a He atom to a He_M cluster as a measure of the stability of He_M clusters in bulk tungsten are shown in figure 1. It can be seen that EAM1 potential shows rapid increase of He binding energy with increasing number of He atoms M in the cluster He_M and significantly overestimates the value of the binding energy as compared to *ab initio* results. At the same time EAM2 and BOP potentials show good agreement with *ab initio* from [21], however with slight underestimation of the binding energy.

The results for incremental binding energy of a H atom to a He_M-H-Vac cluster are shown in figure 2. As can be seen from the figure, the BOP potential overestimates the binding energy almost by a factor of two for clusters containing one to three He atoms. This behaviour of the BOP potential is expected due to the overestimation of the H binding energy to a H_N-Vac cluster [33]. EAM1

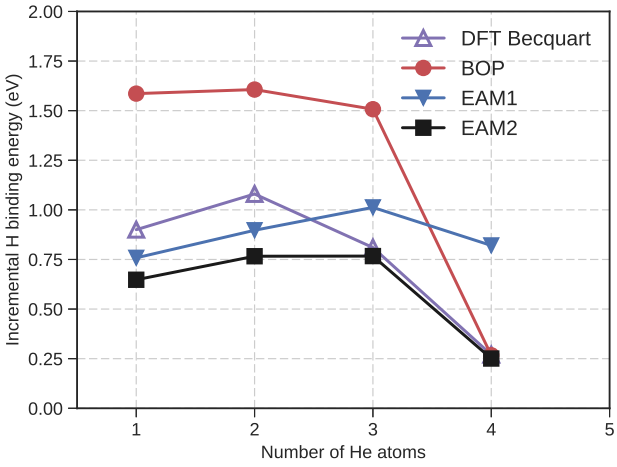

Figure 2: Binding energy of a H atom to a He_M-H-Vac cluster

gives reasonable agreement for clusters with one and two He atoms with an overestimation of the binding energy for bigger clusters, failing to reproduce the *ab initio* trend of the binding energy drop for cluster with four atoms. At the same time the EAM2 potential reproduces the *ab initio* trend well with some underestimations for small clusters.

MS assessment of He_M cluster assisted Frenkel pair formation was made by calculating the energy balance of a system containing a He_M cluster in an ideal W matrix and a system where the same He_M cluster is placed in a vacancy close to a W self-interstitial atom (SIA) (see equation 2). The same energy balance calculations were also performed by DFT techniques in [34]. The results from this work are compared with MS calculations in figure 3. It can be seen that all considered versions of the interatomic potential are in good agreement with the DFT values.

The potentials predict a value for M between five and six atoms as the threshold size of the He_M cluster at which the formation of a Frenkel pair becomes energetically favourable. Despite the significant difference in description of bonding of He_M clusters in bulk tungsten and He_M-H-Vac clusters (see Fig-

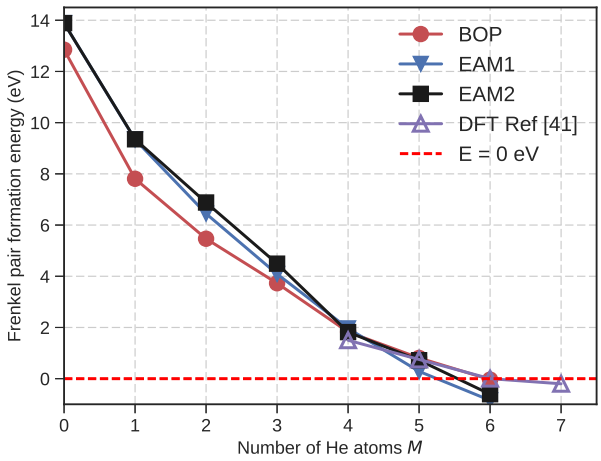

Figure 3: He_M cluster assisted Frenkel pair formation energy

ure 3), both versions of the EAM potentials together with BOP potential give very similar values for the formation energy of Frenkel pairs. Since there is no difference between both EAM and BOP potentials with respect to the He self-trapping mechanism, but the EAM2 potential describes the energetics of He_M and He_M-H-Vac, the EAM2 potential was chosen for the finite temperature simulations.

3.2. Molecular Dynamics results

The results of the first series of MD simulations without He atoms revealing the effect of hydrogen income periodicity (HIP) on hydrogen critical concentration for Frenkel pair formation are shown in figure 4. The value of HIP was varied in the range between 10 to 90 ps/atom and each simulation was repeated 10 times with different initial atom velocity distributions to estimate the uncertainty of hydrogen critical concentration. Due to the small number of the data points, the best way to represent such dataset is so-called box-and-whiskers plot [35]. The box-and-whiskers plot gives an opportunity to visually represent the data distribution properties such as spread and symmetry. The bottom and

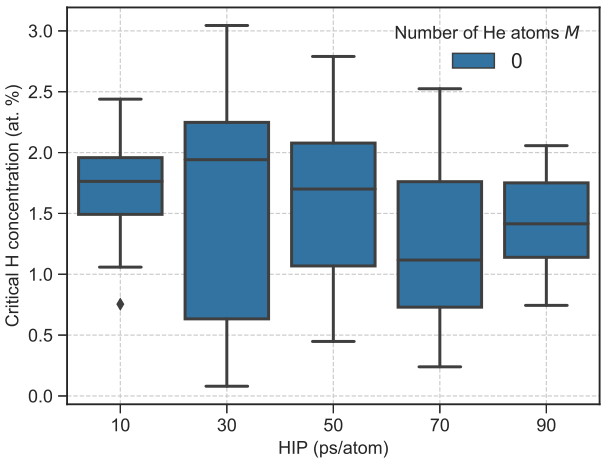

Figure 4: Critical average concentration of H in the absence of He atoms, but in the presence of an initial vacancy.

the top of the box denote the first and the third quartiles correspondingly and thus indicate H-spread or Interquartile Range (IQR), i.e. the range containing 50 % of the values. The line inside the box represents the data median while whiskers span the rest of the dataset. The circles, if present in the graph, show outliers, i.e. the data points that lay further than 1.5×IQR from either the first or the third quartile. As can be seen from the figure, it is not possible to draw any trend in the data as the value of HIP increases, especially taking into account the IQR. Thus it was concluded that the variation of the HIP in the considered range does not affect the value of critical H concentration for Frenkel pair formation in the case of simulations with H only.

As was discussed in the introduction, H and He atoms show significantly different clustering behaviour in bulk tungsten with a strong attraction between He atoms and almost zero interaction between H atoms. Thus one can expect different trapping mechanisms for H and He. Indeed, the qualitative difference can be seen from a visualization of the atomic configurations presented in figure 5. In case of H atoms, an aggregation with the local hydrogen concentration

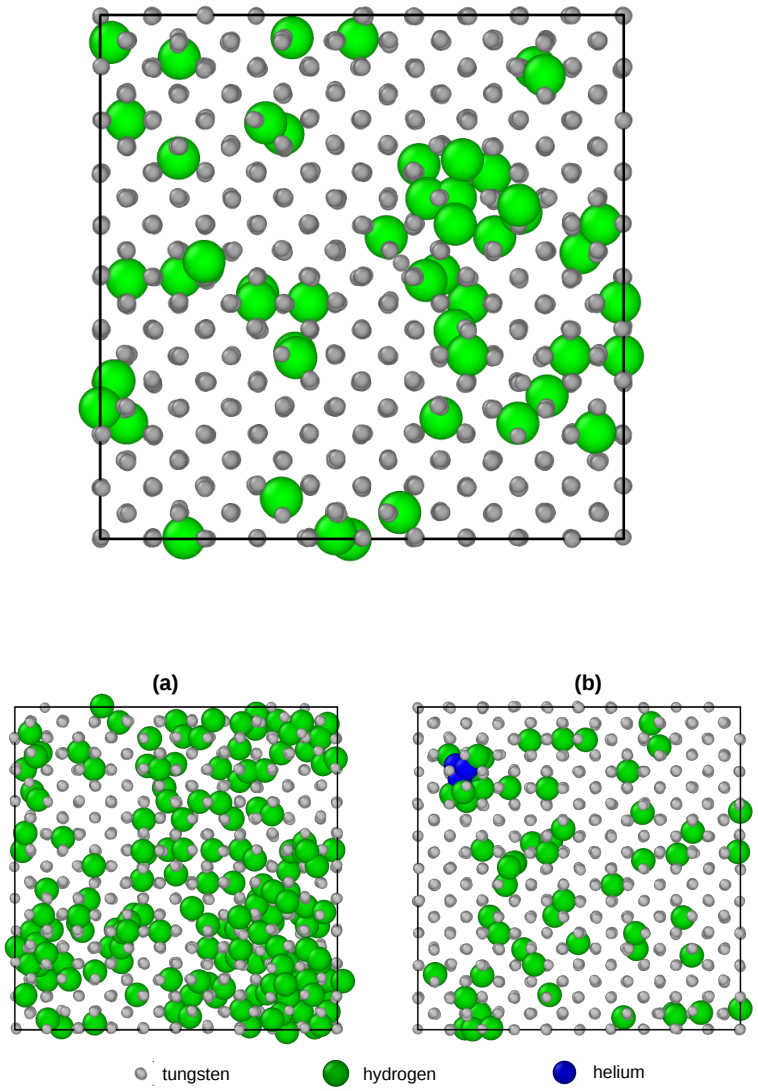

Figure 5: Simulation box snapshots taken at the moment of the first tungsten atom ejection, HIP = 50 ps/atom. Gray - tungsten, green - hydrogen, blue - helium. (top) The crystal with an initial vacancy and no He atoms. The first tungsten atom is ejected at comparatively low concentration of H. (a) A defect-free lattice and no He atoms present. A cloud of H atoms has been formed around the vacant lattice site, the critical average concentration is higher than in (top). (b) A defect-free crystal and three initially present He atoms which have already formed a cluster prior to the W atom ejection.

up to five times higher as compared to the bulk average was formed promoting the W atom ejection within the aggregation volume. At the same time, helium atoms were found to cluster in the very beginning of the simulation, thus causing huge lattice distortion and facilitating the tungsten atom ejection.

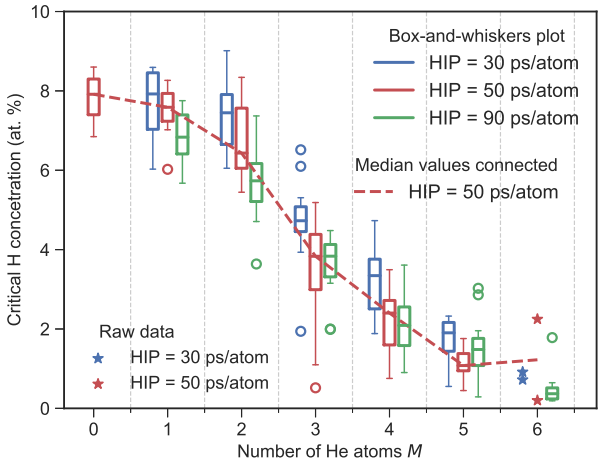

Figure 6: The critical average atomic H concentration variation with the number of He atoms in the W crystal for three values of HIP

The results of the second series of MD simulations revealing the critical H concentration at the moment of the first tungsten atom ejection in the presence of He_M clusters in the system are shown in figure 6. For every considered combination of the initial number of He atoms and HIP the number of successful simulation runs varied from eight to 14 with the exception of simulations with six He atoms with low and middle values of HIP, where the number of successful runs was two. As in the case of pure H simulations and due to the small number of data points, the box-and-whiskers plot [35] was used to represent the data. For the two cases where the number of data points in the dataset was two, the raw data was plotted (coloured stars) since the box-and-whiskers plot for such datasets is misleading. For better visualisation of the trend of critical H concentration evolution, a red dashed line connecting median values for HIP =

50 ps/atom was added.

The results presented in figure 6 show a decrease of the value of critical H concentration with an increase of the number of helium atoms present in the simulation box. The spread of the data allows to estimate the decrease of the critical H concentration approximately by the factor of eight, thus showing the clear evidence of the synergy between hydrogen and helium atoms when they eject a tungsten atom. At the same time the hydrogen income periodicity presented by different colours in the figure has a small effect as it was in case of simulations without He_M clusters (see. figure 4). The fact that the variation of HIP within one order of magnitude does not influence the values for critical H concentration and trapping mechanisms confirms that the results obtained in the simulations can be extrapolated to experimental values of H flux.

The helium atoms were found to bond together at the very beginning of the simulation, thus causing lattice distortion and facilitating the tungsten atom ejection. It was concluded that if more than four He atoms were present in the computation cell, then the tungsten atom ejection was not primarily driven by hydrogen concentration, but by the helium atoms themselves. Thus the presence of small clusters of He atoms in the material during H implantation enhances the H bubble formation. Clusters containing more than four He atoms act as additional traps for H atoms.

So far the main focus of this work was the moment of the first Frenkel pair formation. However it is also important to investigate the subsequent dynamics of bubble formation. The number of detected vacancies as a function of time (bottom X axis) and H concentration (top X axis) for the case of HIP of 50 ps/atom (1 %/ns) is shown in figure 7. The colour of the solid lines shows the number of He atoms M present in the He_M cluster in the system. The dashed vertical lines show the median values for the critical H concentration for formation of the first Frenkel pair - the same data is plotted with red dashed line in figure 6.

As can be seen from the figure, for the simulations with number of He atoms lower than three there is a rapid increase in the rate of the vacancy forma-

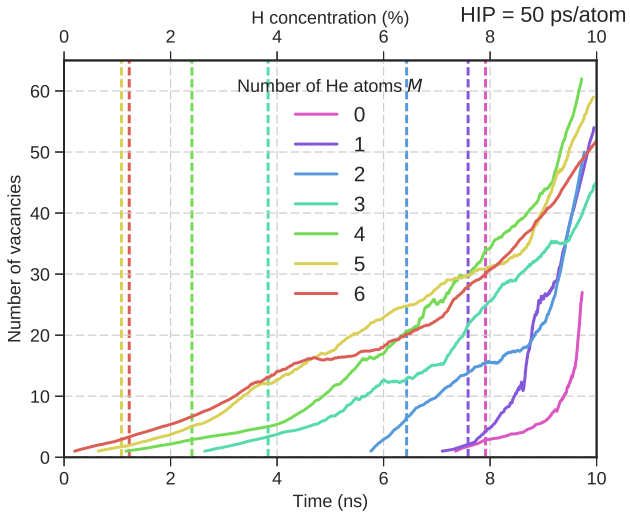

Figure 7: The evolution of the amount of vacancies with time for different number of He atoms present in the simulation. The solid lines represent the vacancy concentration with the colour corresponding to a certain number of He atoms in the cluster. The bottom X axis shows time and the top X axis shows the corresponding H concentration in the system. The results only for HIP = 50 ps/atom (1 %/ns) are shown. Dashed vertical lines represent the median values of critical H concentration for the first Frenkel pair formation and show the same data as the red dashed line in Figure 6

tion (slope of the curve) at the very end of the simulation when the value of the H concentration reaches nine percent. At the same time this effect is less pronounced in the simulations with higher number of He atoms in the system showing a steady increase of the amount of vacancies in the system during the simulations. Moreover in the second part of the simulations, when the H concentration is higher than five percent the curves for six, five and four He atoms show practically identical trends. Thus the presence of He_M clusters in the simulation affects not only the initial Frenkel pair formation mechanism but also the subsequent bubble growth. However, in order to give quantitative estimations of the possible effects one has to perform full scale mean field theory simulations of mixed He-H implantation in the material is needed. Together with our previous study reporting diffusion parameters of He_M and mixed He_M-H_N clusters in W

[25], MS and MD simulations presented in this paper reveal insight about the H assisted Frenkel pair formation mechanism in the presence of He_M clusters and provide the necessary parametrizations for higher scale simulations.

4. Conclusions

A set of MS and MD simulations was performed in order to investigate He and H trapping properties under mixed He-H plasma implantation. Two versions of an EAM potential for the W-H-He system by Bonny *et. al.* [28] in the framework of an EAM model and a BOP potential by Li *et. al.* [26, 27] were validated by comparison of the static calculations with *ab initio* data from the literature. Based on the results of the static simulations the following conclusions can be drawn:

- Results for the stability of He_M clusters revealed that the EAM1 potential shows rapid increase of He binding energy with increase of number of He atoms M in the cluster He_M and significantly overestimates the value of the binding energy as compared to *ab initio* results. At the same time EAM2 and BOP potentials show good agreement.

- Results of the stability of He_M-H-Vac clusters showed that the BOP potential overestimates the binding energy almost by a factor of two for clusters containing one to three He atoms, while both EAM potentials give reasonable agreement.

- Results for the He_M cluster assisted Frenkel pair formation demonstrated that all the considered potentials provide similar values for the formation energy in good agreement with *ab initio* data. However due to the poor performance of the BOP potential regarding the stability of He_M clusters and unsatisfactory results of EAM1 regarding the stability of He_M-H-Vac clusteres, the EAM2 potential was chosen for finite temperature MD simulations.

The effect of He_M cluster size and the H implantation regime (HIP value) on the H bubble formation mechanism in bulk W was investigated by means of MD simulations using the EAM2 potential. As a result of the simulations it is possible to conclude:

- No significant effect on H bubble nucleation mechanism in tungsten was found when H income periodicity was varied from 10 to 90 ps/atom irrespective of the presence of He_M clusters.

- He atoms clustered in the very beginning of the simulations and stayed clustered during the rest of the simulations. The presence of He_M clusters in the material facilitate defect formation by decreasing the critical H concentration needed for Frenkel pair formation and also affects the subsequent bubble growth mechanism.

The performed simulations suggest that the presence of He_M clusters in the material during mixed He-H plasma exposure facilitates H trapping and bubble formation and growth. On top of that, due to the self-trapping mechanism He_M clusters can create vacancies thus being the additional source of traps for H. The results reported in this paper provide a thorough insight into the mechanisms that determine H retention in W in the presence of He in the material that can be used to interpret the results of experiments with both simulatneious [36] and subsequent [37] H and He plasma exposures. However, in order to properly investigate the effect of all the considered mechanisms on the H retention during real experiments one has to perform a full scale mean field theory simulation using the obtained parameterizations. Together with the data for diffusion and thermal stability of mixed He_M-H_N clusters reporter earlier [25], this paper provides the parameters needed for such simulations.

Acknowledgements

This work was supported by the European Commission and carried out within the framework of the Erasmus Mundus International Doctoral College in

Fusion Science and Engineering (FUSION-DC).

References

[1] R. E. Clark, D. Reiter, Nuclear fusion research: understanding plasma-surface interactions, volume 78, Springer, 2005.

[2] R. Joachim, T. Emmanuelle, L. Thierry, P. Volker, B. Sebastijan, L. Alberto, F. C. Glenn, P. D. Russell, S. Klaus, V. O. Olga, A. C. Rion, Tritium inventory in iter plasma-facing materials and tritium removal procedures, Plasma Physics and Controlled Fusion 50 (2008) 103001. URL: http://stacks.iop.org/0741-3335/50/i=10/a=103001.

[3] H. Y. Xu, G. N. Luo, H. Schut, Y. Yuan, B. Q. Fu, A. Godfrey, W. Liu, G. D. Temmerman, Enhanced modification of tungsten surface by nanostructure formation during high flux deuterium plasma exposure, Journal of Nuclear Materials 447 (2014) 22–27. URL: http://www.sciencedirect.com/science/article/pii/S0022311513012968. doi:http://dx.doi.org/10.1016/j.jnucmat.2013.12.010.

[4] J. P. Sharpe, R. D. Kolasinski, M. Shimada, P. Calderoni, R. A. Causey, Retention behavior in tungsten and molybdenum exposed to high fluences of deuterium ions in tpe, Journal of Nuclear Materials 390391 (2009) 709–712. URL: http://www.sciencedirect.com/science/article/pii/S0022311509002153. doi:http://dx.doi.org/10.1016/j.jnucmat.2009.01.195.

[5] W. M. Shu, G. N. Luo, T. Yamanishi, Mechanisms of retention and blistering in near-surface region of tungsten exposed to high flux deuterium plasmas of tens of ev, Journal of Nuclear Materials 367370, Part B (2007) 1463–1467. URL: http://www.sciencedirect.com/science/article/pii/S0022311507006241. doi:http://dx.doi.org/10.1016/j.jnucmat.2007.04.005.

[6] V. K. Alimov, W. M. Shu, J. Roth, K. Sugiyama, S. Lindig, M. Balden, K. Isobe, T. Yamanishi, Surface morphology and deuterium retention in tungsten exposed to low-energy, high flux pure and helium-seeded deuterium plasmas, Physica Scripta 2009 (2009) 014048. URL: http://stacks.iop.org/1402-4896/2009/i=T138/a=014048.

[7] K. Tokunaga, M. J. Baldwin, R. P. Doerner, N. Noda, Y. Kubota, N. Yoshida, T. Sogabe, T. Kato, B. Schedler, Blister formation and deuterium retention on tungsten exposed to low energy and high flux deuterium plasma, Journal of Nuclear Materials 337339 (2005) 887–891. URL: http://www.sciencedirect.com/science/article/pii/S0022311504009298. doi:http://dx.doi.org/10.1016/j.jnucmat.2004.10.137.

[8] L. Buzi, Influence of the Particle Flux on Surface Modifications of Tungsten, Thesis, Université de Lorraine, 2015.

[9] B. Tyburska, Deuterium Retention in Carbon and Self-Implanted Tungsten, Report, Max-Planck-Institut für Plasmaphysik, 2010.

[10] Y. Zayachuk, M. H. J. . t. Hoen, P. A. Z. v. Emmichoven, D. Terentyev, I. Uytdenhouwen, G. v. Oost, Surface modification of tungsten and tungstentantalum alloys exposed to high-flux deuterium plasma and its impact on deuterium retention, Nuclear Fusion 53 (2013) 013013. URL: http://stacks.iop.org/0029-5515/53/i=1/a=013013.

[11] Y. Zayachuk, Deuterium Retention in Tungsten and Tungsten-Tantalum Alloys under High Flux Plasma Exposure ('Deuteriumretentie in wolfraam en wolfraam-tantaallegeringen onder blootstelling aan een hoge plasmaflux'), Thesis, Ghent University, 2013.

[12] M. Baldwin, R. Doerner, Helium induced nanoscopic morphology on tungsten under fusion relevant plasma conditions, Nuclear Fusion 48 (2008) 035001. URL: http://stacks.iop.org/0029-5515/48/i=3/

a=035001?key=crossref.ab90d98340142ce1fd8761231da9d039. doi:10.1088/0029-5515/48/3/035001.

[13] M. J. Baldwin, R. P. Doerner, Formation of helium induced nanostructure 'fuzz' on various tungsten grades, Journal of Nuclear Materials 404 (2010) 165–173. doi:10.1016/j.jnucmat.2010.06.034.

[14] M. Yamagiwa, S. Kajita, N. Ohno, M. Takagi, N. Yoshida, R. Yoshihara, W. Sakaguchi, H. Kurishita, Helium bubble formation on tungsten in dependence of fabrication method, in: Journal of Nuclear Materials, volume 417, 2011, pp. 499–503. doi:10.1016/j.jnucmat.2011.02.007.

[15] Y. Ueda, M. Fukumoto, J. Yoshida, Y. Ohtsuka, R. Akiyoshi, H. Iwakiri, N. Yoshida, Simultaneous irradiation effects of hydrogen and helium ions on tungsten, Journal of Nuclear Materials 386388 (2009) 725–728. URL: http://www.sciencedirect.com/science/article/pii/S0022311508009690. doi:http://dx.doi.org/10.1016/j.jnucmat.2008.12.300.

[16] M. Miyamoto, D. Nishijima, M. J. Baldwin, R. P. Doerner, Y. Ueda, K. Yasunaga, N. Yoshida, K. Ono, Microscopic damage of tungsten exposed to deuteriumhelium mixture plasma in pisces and its impacts on retention property, Journal of Nuclear Materials 415 (2011) S657–S660. URL: http://www.sciencedirect.com/science/article/pii/S0022311511000201. doi:http://dx.doi.org/10.1016/j.jnucmat.2011.01.008.

[17] G.-H. Lu, H.-B. Zhou, C. S. Becquart, A review of modelling and simulation of hydrogen behaviour in tungsten at different scales, Nuclear Fusion 54 (2014) 086001. URL: http://stacks.iop.org/0029-5515/54/i=8/a=086001.

[18] Y.-L. Liu, Y. Zhang, G. N. Luo, G.-H. Lu, Structure, stability and diffusion of hydrogen in tungsten: A first-principles study,

Journal of Nuclear Materials 390391 (2009) 1032–1034. URL: http://www.sciencedirect.com/science/article/pii/S0022311509002918. doi:http://dx.doi.org/10.1016/j.jnucmat.2009.01.277.

[19] K. Heinola, T. Ahlgren, K. Nordlund, J. Keinonen, Hydrogen interaction with point defects in tungsten, Physical Review B: Condensed Matter 82 (2010) 094102. URL: http://link.aps.org/doi/10.1103/PhysRevB.82.094102.

[20] D. F. Johnson, E. A. Carter, Hydrogen in tungsten: Absorption, diffusion, vacancy trapping, and decohesion, Journal of Materials Research 25 (2010) 315–327. URL: http://dx.doi.org/10.1557/JMR.2010.0036. doi:doi:10.1557/JMR.2010.0036.

[21] C. S. Becquart, C. Domain, Migration energy of he in w revisited by ab initio calculations, Physical Review Letters 97 (2006) 196402. URL: http://link.aps.org/doi/10.1103/PhysRevLett.97.196402.

[22] C. S. Becquart, C. Domain, A density functional theory assessment of the clustering behaviour of he and h in tungsten, Journal of Nuclear Materials 386-388 (2009) 109–111. URL: http://www.sciencedirect.com/science/article/pii/S0022311508008179. doi:http://dx.doi.org/10.1016/j.jnucmat.2008.12.085.

[23] H.-B. Zhou, Y.-L. Liu, S. Jin, Y. Zhang, G.-N. Luo, G.-H. Lu, Towards suppressing h blistering by investigating the physical origin of the h-he interaction in w, Nuclear Fusion 50 (2010) 115010. URL: http://stacks.iop.org/0029-5515/50/i=11/a=115010.

[24] A. Takayama, A. M. Ito, Y. Oda, H. Nakamura, First principles investigation of cluster consisting of hydrogenhelium atoms interstitially-trapped in tungsten, Journal of Nuclear Materials 463 (2015) 355–358. URL: http://www.sciencedirect.com/science/article/pii/S002231151400782X. doi:http://dx.doi.org/10.1016/j.jnucmat.2014.11.001.

[25] P. Grigorev, D. Terentyev, G. Bonny, E. E. Zhurkin, G. van Oost, J.-M. Noterdaeme, Mobility of hydrogen-helium clusters in tungsten studied by molecular dynamics, Journal of Nuclear Materials 474 (2016) 143–149. URL: http://linkinghub.elsevier.com/retrieve/pii/S0022311516300952. doi:10.1016/j.jnucmat.2016.03.022.

[26] X.-C. Li, X. Shu, Y.-N. Liu, F. Gao, G.-H. Lu, Modified analytical interatomic potential for a wh system with defects, Journal of Nuclear Materials 408 (2011) 12–17. URL: http://www.sciencedirect.com/science/article/pii/S0022311510006008. doi:http://dx.doi.org/10.1016/j.jnucmat.2010.10.020.

[27] X.-C. Li, X. Shu, Y.-N. Liu, Y. Yu, F. Gao, G.-H. Lu, Analytical whe and hhe interatomic potentials for a whhe system, Journal of Nuclear Materials 426 (2012) 31–37. URL: http://www.sciencedirect.com/science/article/pii/S0022311512001602. doi:http://dx.doi.org/10.1016/j.jnucmat.2012.03.039.

[28] G. Bonny, P. Grigorev, D. Terentyev, On the binding of nanometric hydrogenhelium clusters in tungsten, Journal of Physics: Condensed Matter 26 (2014) 485001. URL: http://stacks.iop.org/0953-8984/26/i=48/a=485001.

[29] M. C. Marinica, V. Lisa, M. R. Gilbert, L. Proville, S. L. Dudarev, J. Marian, G. Bencteux, F. Willaime, Interatomic potentials for modelling radiation defects and dislocations in tungsten, Journal of Physics: Condensed Matter 25 (2013) 395502. URL: http://stacks.iop.org/0953-8984/25/i=39/a=395502.

[30] G. Bonny, D. Terentyev, A. Bakaev, P. Grigorev, D. V. Neck, Many-body central force potentials for tungsten, Modelling and Simulation in Materials Science and Engineering 22 (2014) 053001. URL: http://stacks.iop.org/0965-0393/22/i=5/a=053001.

[31] S. Plimpton, Fast parallel algorithms for short-range molecular dynamics, Journal of Computational Physics 117 (1995) 1 – 19. URL: http://www.sciencedirect.com/science/article/pii/S002199918571039X. doi:http://dx.doi.org/10.1006/jcph.1995.1039.

[32] J. P. Gunn, S. Carpentier-Chouchana, F. Escourbiac, T. Hirai, S. Panayotis, R. A. Pitts, Y. Corre, R. Dejarnac, M. Firdaouss, M. Kočan, M. Komm, A. Kukushkin, P. Languille, M. Missirlian, W. Zhao, G. Zhong, Surface heat loads on the ITER divertor vertical targets, Nuclear Fusion 57 (2017) 46025. URL: http://stacks.iop.org/0029-5515/57/i=4/a=046025.

[33] P. Grigorev, D. Terentyev, G. Bonny, E. E. Zhurkin, G. Van Oost, J. M. Noterdaeme, Interaction of hydrogen with dislocations in tungsten: An atomistic study, Journal of Nuclear Materials 465 (2015) 364–372. URL: http://linkinghub.elsevier.com/retrieve/pii/S0022311515300386. doi:10.1016/j.jnucmat.2015.06.013.

[34] J. Boisse, C. Domain, C. S. Becquart, Modelling self trapping and trap mutation in tungsten using dft and molecular dynamics with an empirical potential based on dft, Journal of Nuclear Materials 455 (2014) 10–15. URL: http://www.sciencedirect.com/science/article/pii/S0022311514001032. doi:http://dx.doi.org/10.1016/j.jnucmat.2014.02.031.

[35] J. W. Tukey, Exploratory data analysis, Adisson-Wesley, New Tork, 1977.

[36] L. Buzi, G. De Temmerman, A. E. Huisman, S. Bardin, T. W. Morgan, M. Rasinski, R. A. Pitts, G. Van Oost, Response of tungsten surfaces to helium and hydrogen plasma exposure under ITER relevant steady state and repetitive transient conditions, Nuclear Fusion 57 (2017). doi:10.1088/1741-4326/aa81e4.

[37] S. Markelj, T. Schwarz-Selinger, A. Založnik, Hydrogen isotope accumula-

tion in the helium implantation zone in tungsten, Nuclear Fusion 57 (2017). doi:10.1088/1741-4326/aa6b27.